Energy flux measurement from the dissipated energy in capillary wave turbulence

Luc Deike, Michael Berhanu, and Eric Falcon
Univ. Paris Diderot, Sorbonne Paris Cité, MSC, UMR 7057 CNRS, F-75 013 Paris, France
(Received 17 September 2013; published 7 February 2014)

We study experimentally the influence of dissipation on stationary capillary wave turbulence on the surface of a liquid by changing its viscosity. We observe that the frequency power-law scaling of the capillary spectrum departs significantly from its theoretical value when the dissipation is increased. The energy dissipated by capillary waves is also measured and found to increase nonlinearly with the mean power injected within the liquid. Here we propose an experimental estimation of the energy flux at every scale of the capillary cascade. The latter is found to be nonconstant through the scales. For fluids of low enough viscosity, we found that both capillary spectrum scalings with the frequency and the newly defined mean energy flux are in good agreement with wave turbulence theory. The Kolmogorov-Zakharov constant is then experimentally estimated and compared to its theoretical value.

DOI: 10.1103/PhysRevE.89.023003 PACS number(s): 47.35.−i, 05.45.−a, 47.52.+j, 47.27.−i

I. INTRODUCTION

When a large ensemble of weakly nonlinear waves interact with each other, they can develop a regime of wave turbulence where the wave energy is transferred from the large forcing scales to the small dissipative scales. Exact solutions of out-of-equilibrium dynamics for the spectral content of energy can be derived analytically by a statistical theory called weak turbulence theory [1,2]. This theory can be applied in various contexts involving waves at various scales: astrophysical plasmas, internal waves in oceanography or in the atmosphere, spin waves in magnetic materials, nonlinear waves in optics, etc. Because of hypotheses of weakly nonlinear waves, infinite systems, local interactions, and scale separations between an energy source and dissipation, the applicability of weak turbulence to real systems can be questionable, and experimental results are often in disagreement with theory (see Refs. [3,4] for recent reviews). In experiments, dissipation is often present at every scale and could explain some of these discrepancies. For instance, the spectrum of wave turbulence on an elastic plate has been experimentally shown to depart from its prediction when dissipation is increased [5], whereas numerical works have shown that the theoretical spectrum is recovered when dissipation within the inertial range is removed [6,7].

Capillary waves are likely the easiest system in which to investigate wave turbulence in the laboratory. Numerous experiments have been dedicated to stationary capillary wave turbulence on the surface of fluids of low viscosity [8–15]. For capillary wave turbulence, weak turbulence theory predicts that the Kolmogorov-Zakharov spectrum of the wave height reads [1]

$$S_\eta(f) = C^{KZ}\epsilon^{1/2}\left(\frac{\gamma}{\rho}\right)^{1/6} f^{-17/6}, \tag{1}$$

where ϵ is the mean energy flux cascading through the scales, γ the surface tension, ρ the liquid density, f the wave frequency, and C^{KZ} the Kolmogorov-Zakharov constant, which can be determined theoretically. Such a frequency scaling $S_\eta \sim f^{-17/6}$ has been observed both numerically [16,17] and experimentally using vibrating plunging wave makers [8,9], vibrating the whole container [10], and working in low-gravity [11] or acoustically levitated [18] environments. With parametric forcing, the capillary wave spectrum displays either peaks and forcing harmonics with maximal amplitudes decreasing roughly as a frequency power law [13–15,19] or a continuum power-law spectrum at much higher frequencies [12,18,20]. Note that this capillary wave turbulence regime driven by nonlinear interactions between waves should not be confused with thermally excited capillary waves that involve only linear mechanisms [21,22].

Some questions still remain open. For instance, experiments show a spectrum scaling with the energy flux in disagreement with the one predicted by theory [8,10,15]. The energy flux is usually estimated by measuring the power injected into the liquid that is assumed to be transferred in the wave system without dissipation within the inertial range. Another attempt to estimate the mean energy flux consists of measuring the wave energy decay rate after switching off the wave maker [23]. However, in an earlier paper [24], we have experimentally shown that the energy decay in gravity-capillary wave turbulence is mainly piloted by large-scale viscous dissipation.

In this paper we will study stationary gravity-capillary wave turbulence on the surface of liquids of different viscosities. We show that the frequency scaling of the capillary spectrum departs from its theoretical prediction when dissipation is increased. By measuring the power injected to the liquid, together with the dissipated powers by gravity and capillary waves, we show that most of the injected energy is dissipated at large scales by gravity waves, whereas a small part feeds the capillary cascade. Moreover, the energy dissipated by capillary waves is found to increase nonlinearly with the mean injected power. Both results mean that estimating the mean energy flux in the capillary cascade by the injected power is not valid. Here we propose an original estimation of the energy flux at every scale of the capillary cascade from the experimental energy spectrum and the wave dissipation rate. This energy flux is then found to be nonconstant through the capillary scales in contrast to the assumptions. However, defining a mean energy flux over the scales allows us to rescale the wave spectrum with the mean energy flux in good agreement with wave turbulence theory for fluids of low enough viscosity. The Kolmogorov-Zakharov constant is then evaluated experimentally, for the first time.

The paper is organized as follows. In Sec. II we recall the origin of wave dissipation in wave turbulence on the surface of a liquid. The experimental setup is described in Sec. III. The

experimental results are then discussed: the evolution of the wave spectrum when the dissipation is increased (Sec. IV), the measurement of the dissipated powers by gravity and capillary waves, and their corresponding spectra (Sec. V). Finally, we present the experimental estimation of the energy flux at every scale (Sec. VI) and of the Kolmogorov-Zakharov constant (Sec. VII). A conclusion is given in Sec. VIII.

II. ORIGIN OF WAVE DISSIPATION

Dissipation of propagating waves in a closed basin has been studied theoretically and experimentally by various authors [25–27]. Linear viscous dissipation leads to an exponential decay of the wave: $\eta(t) = \eta_0 e^{-\Gamma t}$, with η_0 the initial amplitude of the wave and Γ^{-1} its theoretical damping time, which depends on the frequency and the nature of dissipation. Wave damping can have different origins: bottom boundary layer (Γ_B), side wall boundary layer (Γ_W), and surface dissipation. Two types of surface dissipation can be considered: the classical viscous dissipation at a free surface $\Gamma_\nu \sim \nu k^2$ [26,27] or viscous dissipation in the presence of an inextensible film $\Gamma_S \sim (\nu f)^{1/2} k$ [25,27]. The latter comes from the presence of surfactants or contaminants at the interface that leads to an inextensible surface where the tangential velocity is canceled at the interface and was first considered to study the effect of the calming effect of oil on water. Note that these surface dissipations are incompatible since they correspond to two different kinematic conditions at the interface [27]. The decay rate for the wave of frequency f is defined by $\delta \equiv \Gamma/(2\pi f)$. The theoretical decay rate for the various types of viscous dissipation in a liquid of arbitrary depth h are [25–27]

$$\delta_\nu = \frac{\nu k^2}{\pi f}, \tag{2}$$

$$\delta_S = \left(\frac{\nu}{4\pi f}\right)^{1/2} \frac{k \cosh^2 kh}{\sinh 2kh}, \tag{3}$$

$$\delta_B = \left(\frac{\nu}{4\pi f}\right)^{1/2} \frac{k}{\sinh 2kh}, \tag{4}$$

$$\delta_W = \left(\frac{\nu}{4\pi f}\right)^{1/2} \frac{1}{2R}\left[\frac{1+(m/kR)}{1-(m/kR)} - \frac{2kh}{\sinh 2kh}\right], \tag{5}$$

where R is the size of the circular vessel, and $m = 1$ the antisymmetrical modes and $m = 0$ the symmetrical ones.

In an earlier paper [24], we have experimentally shown that the major part of dissipation occurs at large scales in gravity-capillary wave turbulence, and that the experimental decay rate scales as $\nu^{1/2}$ over two decades in viscosity, and not as ν^1 as expected by classical viscous dissipation. In our experiments, viscous dissipations by the surface boundary layer and bottom boundary layer are the most important, while friction at the lateral boundary is negligible [24]. Bottom friction is significant at a large scale since the forcing scales are of the order of the depth. The experimental wave dissipation is correctly described by the total theoretical dissipation:

$$\Gamma(f) = 2\pi f \delta_T = 2\pi f(\delta_S + \delta_B + \delta_W). \tag{6}$$

The fact that the inextensible condition has to be taken into account instead of the usual free surface condition was previously observed in laboratory experiments with water [25,28,29]. Indeed, if no particular attention is paid (such as working in clean rooms, filtered liquids, or liquids with low enough surface tension), the surface dissipation by boundary layer dominates the νk^2 dissipation [29]. Finally, note that the infinite depth condition is satisfied for $f > 10$ Hz (i.e., $\lambda < 2$ cm and $kh \gg 1$), and thus bottom friction becomes negligible also for capillary waves. Consequently, in our experiments, the dissipation source for capillary waves is only due to surface dissipation in the presence of an inextensible film [24]. In the following, we will estimate the damping rate using the full Eq. (6) since gravity and capillary waves are involved in our experiments.

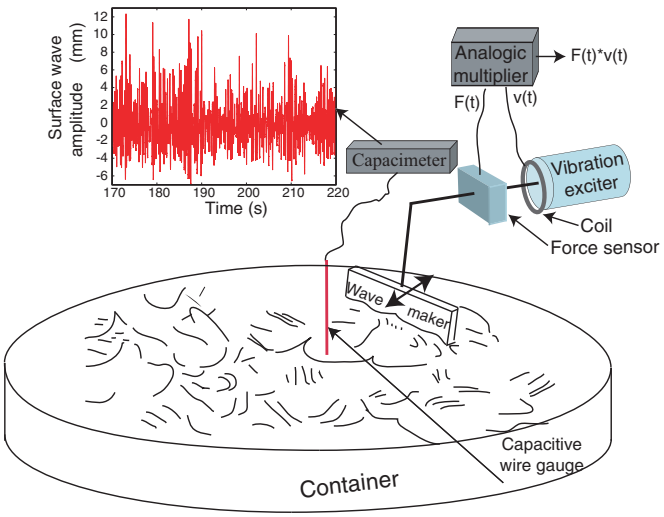

FIG. 1. (Color online) Experimental setup. The diameter of the vessel is 22 cm.

III. EXPERIMENTAL SETUP

The experimental setup is shown on Fig. 1, is the same as in the experiment on freely decaying wave turbulence [24] and similar to the one used in Ref. [8]. It consists of a circular plastic vessel, 22 cm in diameter, filled with a liquid to a height $h = 25$ mm. Various liquids are used: water, mercury, silicon oils, and aqueous solutions of glycerol (denoted as $x\%$ GW with x the glycerol percentage) to vary kinematic viscosity, ν, over two orders of magnitude. Properties of these liquids are listed in Table I. The main difference between the different fluids

TABLE I. Physical liquid properties: density, ρ, kinematic viscosity, ν, and surface tension γ [30]. The frequency transition between gravity and capillary waves is f_{gc} (see text).

Liquid	ρ (kg/m^3)	ν (m^2/s)	γ (mN/m)	f_{gc} (Hz)
Mercury	13 600	1.1×10^{-7}	400	17
Water	1000	10^{-6}	73	14
20% glycerol-water	1020	2×10^{-6}	70	13.5
30% glycerol-water	1050	3×10^{-6}	70	14
50% glycerol-water	1120	5×10^{-6}	68	14
Silicon oil V5	1000	5×10^{-6}	20	18.8
Silicon oil V10	1000	10^{-5}	20	18.5

is their kinematic viscosity. The theoretical gravity-capillary transition $f_{gc} = \frac{1}{2\pi}\sqrt{2g/l_c}$ is between 14 and 19 Hz in all cases, with $l_c = \sqrt{\gamma/(\rho g)}$ the capillary length, ρ the density, and γ the surface tension.

Surface waves are generated by a rectangular plunging wave maker (13 cm in length and 3.5 cm in height) driven by an electromagnetic vibration exciter (LDS V406) driven by a random noise (in amplitude and frequency) band-pass filtered typically between 0.1 and 5 Hz. The wave maker is continuously driven, and the wave height $\eta(t)$ is recorded during the stationary regime (300 s acquisition time) at a given location (center of the vessel) by a capacitive wire gauge plunging perpendicularly to the liquid at rest [8,24]. The capacitive gauge is calibrated for each liquid, and we have checked than the response is linear with the wave height whatever the working liquid.

The force $F(t)$ applied by the shaker to the wave maker and the velocity $V(t)$ of the wave maker are measured to access the injected power $I = F \times V$ into the liquid [8]. We have checked that the classical relation $\langle I\rangle \sim \rho\sigma_V^2$ [8,31] between the wave maker rms velocity and the mean injected power holds for every liquid. Moreover, a scaling $\langle I\rangle \sim \nu^{1/2}$ is observed, compatible with the observed dissipation. One also observes $\langle I\rangle/\rho \sim \sigma_\eta^2$ for all liquids, which is due to the fact that the gravity wave energy scales as $\sim g\eta^2$. The mean injected power value is thus directly related to the rms wave height. $\langle I\rangle$ is normalized by ρ and the vessel surface $S = \pi R^2$ to compare the results without considering the inertial effects

$$\epsilon_I = \frac{\langle I\rangle}{\rho S}\,. \tag{7}$$

ϵ_I has thus the dimension of an energy flux by density unit ($[L^3T^{-3}]$), as for the theoretical mean energy flux ϵ.

IV. ROLE OF DISSIPATION IN CAPILLARY WAVE TURBURLENCE

In this section we investigate the influence of an increasing dissipation on capillary wave turbulence.

A. Power spectrum of wave height

We first focus on the power spectrum of wave height, $S_\eta(f)$, on the surface of various liquids of different viscosities. Figure 2 shows $S_\eta(f)$ for different viscosities ($1.1 \times 10^{-7} \leqslant \nu \leqslant 5 \times 10^{-5}$ m^2/s) and different forcing amplitudes.

For *low dissipation* (i.e., small viscosity as in mercury or water), $S_\eta(f)$ displays two frequency power laws whatever the forcing amplitude [see Fig. 2(a)], corresponding to the gravity (6 Hz $< f < f_{gc}$) and capillary ($f_{gc} < f \lesssim 120$ Hz) wave turbulence regimes. The transition between these two regimes is observed around the theoretical gravity-capillary transition frequency f_{gc}. The gravity spectrum scales as $S_\eta^g \sim f^{-\beta}$, where β is found to increase (from 4.5 to 5.5) with the injected power as previously found in tanks of various sizes [8,23,32–34]. It thus differs from the forcing-independent exponent of the Kolmogorv-Zakharov spectrum ($\sim f^{-4}$) [35] or the Phillips spectrum ($\sim f^{-5}$) [36]. The observed dependence could be due to possible finite size effects, but no direct comparison exists with models including these effects [37–40]. Within the capillary inertial range ($f_{gc} < f \lesssim 120$ Hz), one has $S_\eta \sim f^{-\alpha}$, with $\alpha = 2.8 \pm 0.2$ independent of the injected

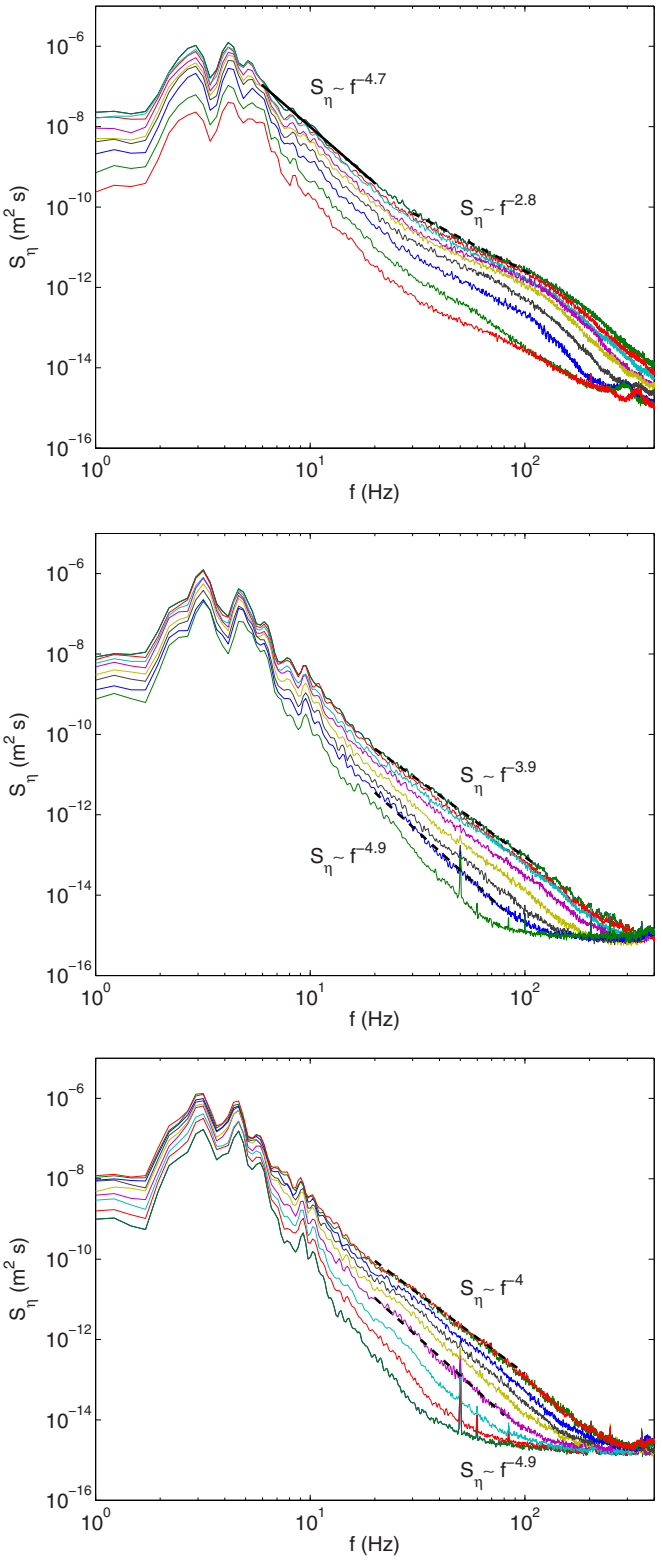

FIG. 2. (Color online) Power spectrum $S_\eta(f)$ for low (top), medium (middle), and high (bottom) viscosity corresponding respectively to mercury, 30% GW, and 50% GW of viscosity $\nu = 1.1 \times 10^{-7}$, 3×10^{-6}, and 5×10^{-6} m^2/s. Injected power increases from bottom to top. Dashed lines are power law fits.

power, and in good agreement with wave turbulence theory ($\sim f^{-17/6}$). At higher frequencies ($f > f_d \approx 120$ Hz), the spectrum shape changes due to an increase of dissipation. All these results are similar to those found in Refs. [8,24].

For higher viscosities ($\nu > 2 \times 10^{-6}$ m^2/s), the spectrum phenomenology changes as shown in Figs. 2(b)–2(c). It is not possible anymore to define a cascade within the gravity wave range; the power law has been replaced by peaks, corresponding to the vessel eigenvalues and their harmonics. However, a power law is still observed in the capillary wave range, $S_\eta \sim f^{-\alpha}$, with α larger than its theoretical value and dependent on the injected power. The wave spectrum is steeper when the injected power decreases. These observations are valid for all considered liquids with $\nu > 2 \times 10^{-6}$ m^2/s, both in aqueous solutions of glycerol and in silicon oil. We will refer below this behavior as the *high dissipation* regime of wave turbulence. Finally, when the viscosity is increased, a change of curvature of spectrum shapes is observed near high frequencies ($f \gtrsim 120$ Hz) in Fig. 2. For high enough viscosity, the capillary cascade gets directly into the noise level, which can be ascribed to the lower sensitivity of the capacitive gauge when the glycerol concentration is increased.

B. Frequency power-law exponent of the spectrum

Figure 3 shows $S_\eta(f)$ at different kinematic viscosities for a fixed strong forcing. For the two lowest viscosity liquids, the spectrum exhibits two frequency power laws, corresponding to the gravity wave cascade, $S_\eta(f) \sim f^{-5\pm0.5}$, and the capillary one $S_\eta(f) \sim f^{-2.8}$. Thus at *low dissipation*, the capillary exponent is in good agreement with the wave turbulence prediction. When the dissipation is increased, a capillary cascade is still observed, $S_\eta(f) \sim f^{-\alpha}$, but with an exponent α dependent on the viscosity as shown in the inset of Fig. 4.

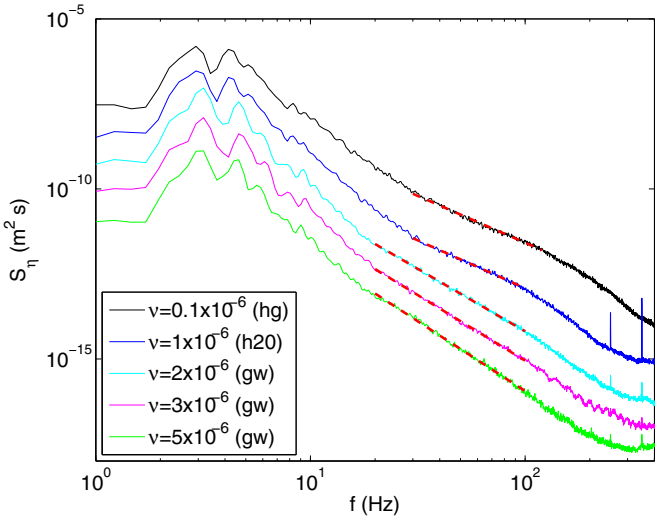

FIG. 3. (Color online) $S_\eta(f)$ for various liquids: mercury, water, 20% GW, 30% GW, and 50% GW ($\nu = 1.1 \times 10^{-7}$, 10^{-6}, 2×10^{-6}, 3×10^{-6}, and 5×10^{-6} m^2/s, from top to bottom). $\epsilon_I \approx 5 \times 10^{-5}$ m^3 s^{-3}. Curves are shifted vertically for clarity by a factor 1, 0.5, 0.1, 0.01, and 0.001, respectively. Dotted (red) lines show best power-law fits, $S_\eta \sim f^{-\alpha}$, with α =2.8, 2.8, 3.7, 3.9, and 4.1 (from top to bottom).

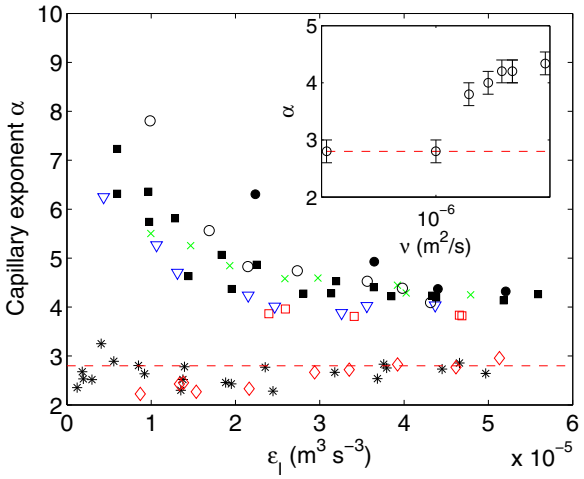

FIG. 4. (Color online) Main: Capillary exponent α as a function of ϵ_I for various liquids $\nu = 1.1 \times 10^{-7}$ (∗), 10^{-6} (◇), 2×10^{-6} (□), 3×10^{-6} (▽), 4×10^{-6} (×), 5×10^{-6} (GW) (■), 5×10^{-6} (oil) (●), and 10^{-5} m^2/s (○). Inset: α vs ν for fixed forcing $\epsilon_I \approx 5 \times 10^{-5}$ m^3 s^{-3}. The theoretical capillary exponent $\alpha = 17/6$ is indicated by dashed (red) lines.

Figure 4 shows the capillary exponent α as a function of ϵ_I. At low viscosity ($\nu \leqslant 10^{-6}$ m^2/s), the exponent $\alpha = 2.8 \pm 0.2$, independent of ϵ_I, as expected by the theory. At higher viscosity ($\nu \geqslant 2\ 10^{-6}$ m^2/s), α is larger than the theoretical value and depends on the injected power: α decreases with ϵ_I up to a saturating value at large forcing ($\epsilon_I > 3\ 10^{-5}$ m^3 s^{-3}).

C. Discussion

The capillary cascade displays two qualitative behaviors regarding the amount of dissipation. When the dissipation is low enough, the theoretical scaling in frequency is observed and is independent of the injected power, as previously reported. When the dissipation is increased beyond a certain point, a steeper power-law spectrum is observed. This discrepancy between theory and experiment becomes larger when the dissipation is further amplified. This result is very similar to the one recently reported in flexural wave turbulence [5]. Moreover, the frequency exponent of the wave spectrum power law depends on the injected power. This latter reminds us of what is observed in gravity wave turbulence [8,23,34]. Recent results in hydroelastic wave turbulence on the surface of a floating elastic sheet [41] also show a wave turbulence regime with a power law steeper than the one given by theoretical predictions. Dissipation could be also responsible of this dependency in those systems. Note that finite size effects on capillary wave turbulence have been described numerically [42] but should not be relevant in our case since capillary waves are damped before experiencing multiple reflexions with vessel boundaries.

V. EXPERIMENTAL DETERMINATION OF DISSIPATED POWER BY THE WAVES

The part of the injected power linearly dissipated by the waves will now be determined experimentally, using the experimental wave height spectrum $S_\eta(f)$ and the theoretical

dissipation rate $\Gamma(f)$, and will be compared to the mean injected power at the wave maker ϵ_I.

A. Definitions

The potential wave energy, per surface, and density unit is $E_g = \frac{1}{2}g\eta^2$ for gravity waves and by $E_c = \frac{1}{2}\frac{\gamma}{\rho}k^2\eta^2$ for capillary waves. For linear waves, the total energy is given by the sum of the kinetic and the potential terms, and both values are equal in average. Since we do not measure the kinetic energy, the potential energy is multiplied by 2 to take into account the kinetic energy. The wave energy spectrum in the Fourier space E_f is related to the total energy $E = \int E_f\, df$ where $E_f = E_f^g + E_f^c$, and to the wave height power spectrum $S_\eta(f)$ by

$$E_f^g(f) = gS_\eta(f), \text{ for gravity waves,} \tag{8}$$

$$E_f^c(f) = \frac{\gamma}{\rho}k^2 S_\eta(f), \text{ for capillary waves.} \tag{9}$$

We define the wave dissipation spectrum $D_\eta(f)$ by

$$D_\eta(f) = E_f(f)\Gamma(f), \tag{10}$$

where $E_f(f)$ is the wave energy spectrum and $\Gamma = 1/\mathcal{T}$ the theoretical dissipation rate of Eq. (6). $D_\eta(f)$ can be split into two terms, the capillary wave dissipation spectrum and the gravity one, with $D_\eta(f) = D_\eta^g(f) + D_\eta^c(f)$ and

$$D_\eta^g(f) = gS_\eta(f)\Gamma(f), \tag{11}$$

$$D_\eta^c(f) = \frac{\gamma}{\rho}k^2 S_\eta(f)\Gamma(f). \tag{12}$$

The total power dissipated linearly by the waves is then given by integrating the dissipation spectrum:

$$D = \int D_\eta(f)\, df = \int E_f(f)\Gamma(f)\, df, \tag{13}$$

The capillary and gravity dissipated powers are separately calculated:

$$D_g = \int_{f_T}^{f_{gc}} gS_\eta(f)\Gamma(f)\, df, \tag{14}$$

$$D_c = \int_{f_{gc}}^{f_s/2} \frac{\gamma}{\rho}k^2 S_\eta(f)\Gamma(f)\, df, \tag{15}$$

and the integration ranges are given by $f_T = 1/T$, the lowest accessible frequency where $T = 300$ s is the total measurement time, f_{gc} the gravity-capillary transition, and f_s is the sampling frequency ($f_s = 1$ kHz). The total power dissipated by the waves is given by $D = D_c + D_g$. Thus, if all the injected power by the wave maker goes into the waves, we should have the power budget

$$\epsilon_I \equiv \frac{\langle I\rangle}{\rho S} = D = D_g + D_c. \tag{16}$$

The dimension of ϵ_I, D, D_c, and D_g is $[L^3T^{-3}]$, the same as the one of the energy flux of wave turbulence theory. Note that this power budget does not take into account wave dissipation by nonlinear processes or bulk dissipation (the fluid being supposed to be almost irrotational, and all the dissipation takes place near the boundaries).

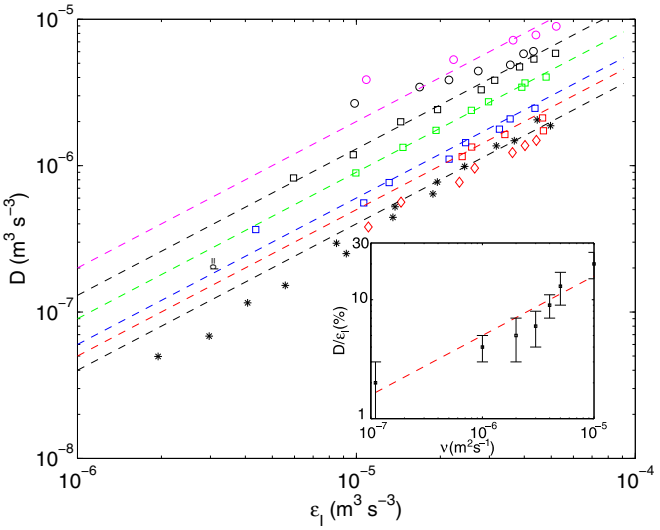

FIG. 5. (Color online) Main: Power dissipated by the waves D as a function of ϵ_I for different fluids (ν increases from bottom to top). Symbols are the same as in Fig. 4. Dashed lines are linear fits $D = p(\nu)\epsilon_I$. Inset: Part of the injected power dissipated in waves $p = D/\epsilon_I$ (in %) as a function of ν. Dashed line is the best fit $p \sim \nu^{1/2}$.

B. Dissipated power by the waves

We first measure the total power dissipated by the waves, D, from the experimental power spectrum, $S_\eta(f)$, and using Eqs. (13), (8), and (9). Figure 5 shows that D increases roughly linearly with ϵ_I for all fluids with a slope p that depends on ν. The inset of Fig. 5 shows that $p \sim \nu^{1/2}$ as expected by the definition $D \sim \Gamma$ [see Eq. (13)] and by the nature of dissipation $\Gamma \sim \nu^{1/2}$ (see Sec. II). To sum up, Fig. 5 shows that the power dissipated linearly by the waves is proportional to the mean injected power $D \sim \epsilon_I$. However, only a small part of the injected power is linearly dissipated by the waves. Indeed, the inset of Fig. 5, shows that $p = D/\epsilon_I$ is only around 5% in mercury and grows to ≈13% in the GW solutions and up to around 20% in silicon oils. We will discuss later the possible mechanisms responsible for these observations.

The dissipated power budget is shown in Fig. 6 in the case of low dissipation (mercury) and high dissipation (GW 50%). The total power dissipated D and the parts dissipated by gravity waves, D_g, and by capillary waves, D_c, are computed from the experimental power spectrum, $S_\eta(f)$, and using Eqs. (13), (14), and (15). In both dissipation cases, the power dissipated by gravity waves is much larger than the one by capillary waves. Moreover, D_g is roughly linear with ϵ_I, whereas D_c is found to scale nonlinearly with ϵ_I (e.g., $\sim \epsilon_I^2$ for mercury at high ϵ_I). As explained below, this result will be of prime interest to understanding the scaling of $S_\eta(f)$ with the energy flux.

Calculating the ratio D_g/D as a function of ϵ_I shows that 65%–85% of the wave dissipated power is dissipated by the gravity waves for mercury and 95%–85% for GW fluids. Thus, not more than 35% of the dissipated power is due to capillary waves for mercury and less than 15% for GW fluids.

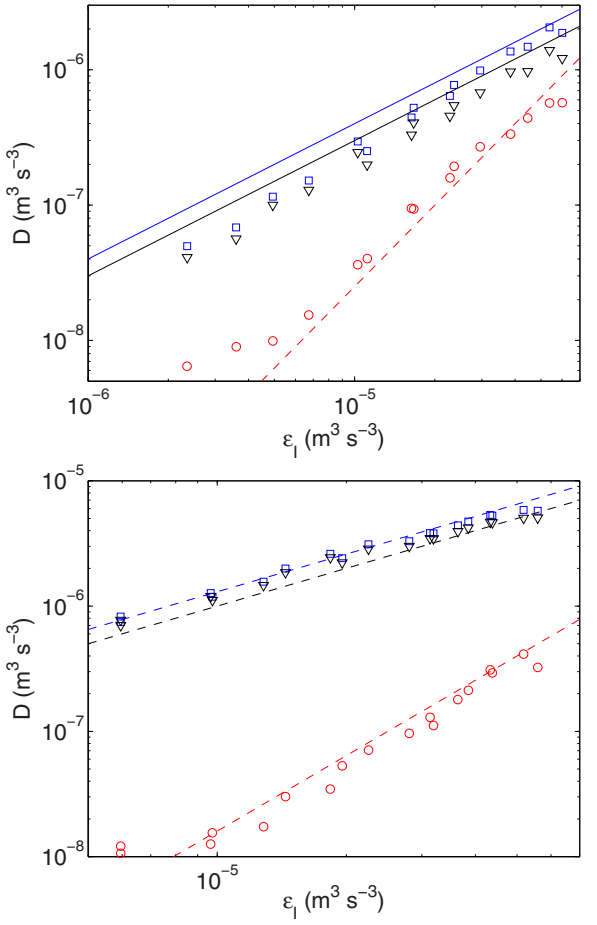

FIG. 6. (Color online) Power dissipated by waves, (□): D, (○): D_c, and (▽): D_g as a function of ϵ_I, for mercury (top) and GW 50% (bottom). Solid lines are linear fits. Dashed lines show the fit $D_c \sim \epsilon_I^2$. Most of the wave dissipation is done by gravity waves.

C. Wave dissipation spectrum

The spectrum of wave dissipation, $D_\eta(f)$, is obtained from the experimental power spectrum of wave height, $S_\eta(f)$, and using Eqs. (10), (9), (8), and (6). Figure 7 shows $D_\eta(f)$ as a function of frequency, in the case of low dissipation (mercury) and high dissipation (GW 50%). The dissipation spectrum of gravity waves, $D_\eta^g(f)$, and of capillary waves, $D_\eta^c(f)$, are computed from $S_\eta(f)$ and using Eqs. (11), (12), and (6). In both dissipation cases, Fig. 7 shows that most dissipation occurs at large scales within the gravity wave frequency range, near the forcing scales. D_η^g declines then abruptly at higher frequency. Note that the shape of D_η^c is very different in the case of low and high dissipation. For low dissipation, a capillary cascade is observed in good agreement with wave turbulence theory [see inset of Fig. 7 (top)], and D_η^c remains large at all scales: D_η^c is almost constant within the capillary inertial range ($f_{gc} \lesssim f \lesssim f_d \approx 120$ Hz), before slightly increasing ($f_d \approx 120$ Hz), and decreasing abruptly after the end of the capillary cascade. For high dissipation, energy is also dissipated at all scales, but the amplitude of D_η^c decreases much more faster in frequency as a consequence of a much steeper wave height power spectrum.

The theoretical frequency scaling of the dissipation spectrum of capillary waves is easily determined by combining

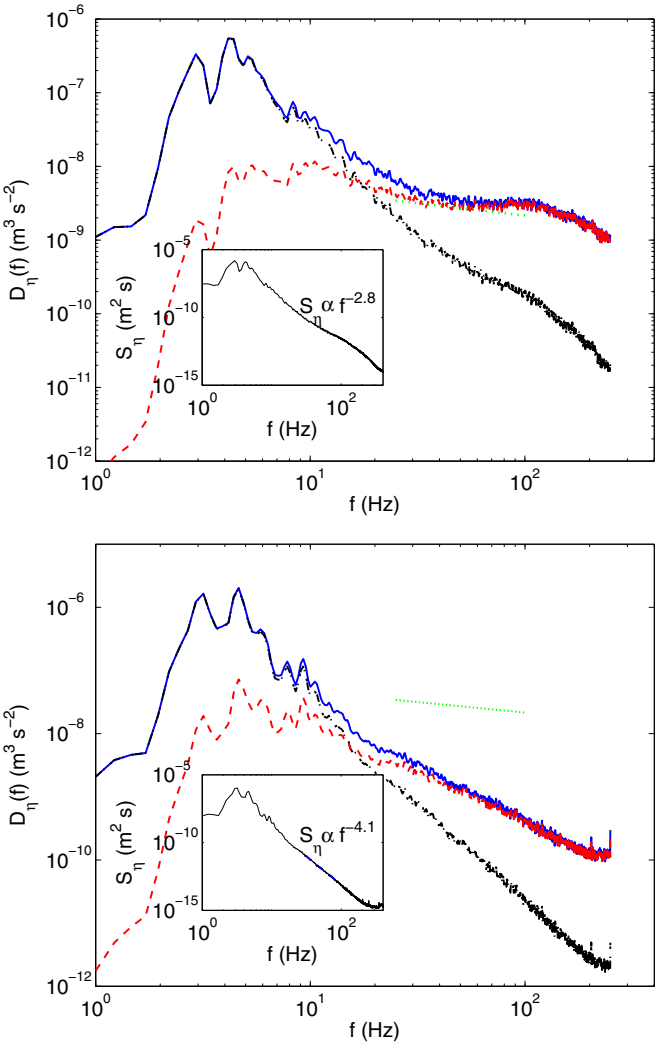

FIG. 7. (Color online) Spectrum of wave dissipation. Mercury (top), 50% GW fluid (bottom). From top to bottom: Total dissipation spectra $D_\eta(f)$ (blue solid line), of pure gravity waves $D_\eta^g(f)$ (black dot dashed line), and of pure capillary waves $D_\eta^c(f)$ (red dashed line). Dotted line shows the theoretical scaling $D_\eta^c \sim f^{-1/3}$. Inset: Corresponding spectrum of wave height $S_\eta(f)$, where $f^{-2.8}$ (top) and $f^{-4.1}$ (bottom) are the best fits in the capillary range.

the Kolmogorv-Zakharov solution of Eq. (1), $S_\eta \sim f^{-17/6}$, and the dissipation rate, from Eq. (3), $\Gamma \sim f^{1/2}k$. Using the capillary wave dispersion relation $\omega^2 \sim k^3$, we then obtain $D_\eta^c \sim S_\eta \Gamma \sim f^{-1/3}$. For low dissipation, we observe that D_η^c is almost constant within the capillary inertial range ($f_{gc} < f < f_d$) as shown in Fig. 7 (top), and so in rough agreement with the $f^{-1/3}$ prediction. For high dissipation, D_η^c is far from this theoretical scaling [see Fig. 7 (bottom)], $S_\eta(f)$ being also much steeper than the theoretical wave spectrum (see inset).

D. Dissipation at all scales

In this part we have experimentally determined the dissipated power in capillary and gravity waves and their corresponding spectra. We have shown quantitatively that dissipation occurs at all scales, and that only a small part

of the power injected by the wave maker is linearly dissipated by waves. The main part must therefore be dissipated either in the bulk or by nonlinear wave dissipation processes (that are not taken into account in the present estimation of the wave dissipation) such as wave breakings [43,44] or the formation of capillary ripples on crested gravity waves [45–47].

We have also shown that the wave energy is mainly dissipated by gravity waves and that only a small part is transferred to capillary waves. In consequence, the capillary wave turbulence cascade is fed by only a small amount of the energy contained in the gravity waves, as discussed in Ref. [24]. Moreover, the dissipated power by capillary waves has been found to scale nonlinearly with ϵ_I, at high enough injected power. Thus, the energy cascading through the capillary cascade is not proportional to the injected power. Instead of ϵ_I, we will now define a quantity representing better the mean energy flux cascading through the capillary scales.

VI. ESTIMATION OF THE ENERGY FLUX

We will focus here on our experiments performed at *low dissipation* in which the frequency scaling of the experimental spectrum is found in agreement with the theoretical one of Eq. (1). Let us discuss now the spectrum scaling with the mean energy flux ϵ. To do that, two experimental estimations of ϵ are used.

First, ϵ is estimated straightforwardly by the mean injected power, $\epsilon \equiv \epsilon_I$, as previously proposed in Refs. [8,15]. This estimation assumes that all the power injected into the system is injected into waves, then transferred through the gravity and capillary scales without dissipation, and finally dissipated at the end of the capillary cascade. The spectra of Fig. 2 (top) normalized by ϵ_I^1 displays a good collapse on a single curve as shown in Fig. 9. However, as also reported previously [8,15], this $S_\eta \sim \epsilon_I^1$ scaling is in disagreement with the predicted one of Eq. (1) of weak turbulence theory. This discrepancy is explained by the presence of dissipation at all scales. Indeed, the mean injected power ϵ_I is not a good estimation of the energy flux within the capillary cascade since the energy dissipated by the capillary wave is not linearly dependent of ϵ_I as shown in Sec. V.

A better way to estimate the energy flux is from the dissipated power by the capillary waves. The total power dissipated linearly by the capillary wave is given by Eq. (15), that is, $D_c = \int_{f_{gc}}^{f_s/2} D_\eta^c(f)\,df$. This quantity integrates the power dissipated within the capillary cascade but also within the dissipative part of the spectrum. Thus, estimating $\epsilon \equiv D_c$ would lead to an overestimation of the mean energy flux. The power budget in the frequency Fourier space reads [2,7]

$$\frac{\partial E_f}{\partial t} = -\frac{\partial \epsilon(f)}{\partial f}. \tag{17}$$

Consequently, the energy flux $\epsilon(f^*)$ at a given frequency f^* reads

$$\epsilon(f^*) = \int_{f^*}^{f_s/2} D_\eta^c(f)\,df. \tag{18}$$

In practice, $\epsilon(f^*)$ is obtained using Eqs. (12), (6), and (18) and the experimental power spectrum of wave height, $S_\eta(f)$.

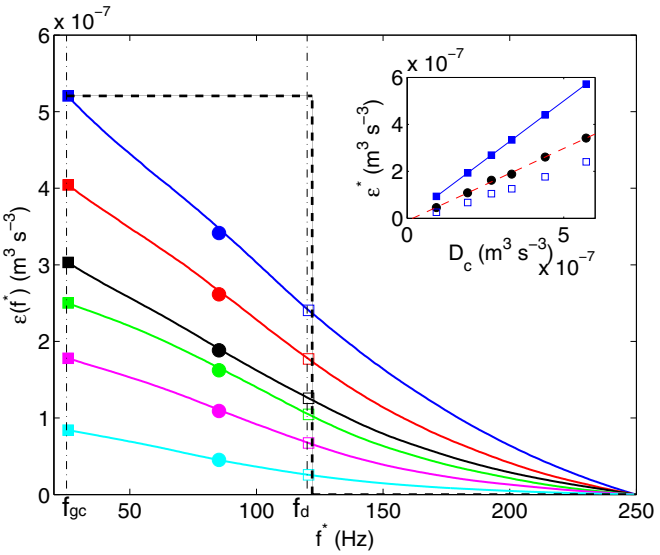

FIG. 8. (Color online) Experimental energy flux $\epsilon(f^*)$ at frequency f^* estimated from Eq. (18) for an increasing forcing amplitude (from bottom to top). Mean energy flux ϵ^* (•) estimated from Eq. (19), energy flux at f_{gc} [$\epsilon(f_{gc}) = D_c$ (■)] and at f_d [$\epsilon(f_d)$ (□)]. Same data as in Fig. 2 (top). Vertical dot-dashed lines indicate f_{gc} and f_d delimiting the frequency range of the capillary cascade. Dashed lines: Theoretical scenario of a constant flux in the inertial range and dissipation localized at f_d. Inset: Same symbols as in the main figure as a function of the dissipated power by capillary waves D_c. Dashed line is a linear fit. Solid line has a unit slope.

Figure 8 shows $\epsilon(f^*)$ as a function of the frequency f^* within the capillary range and for various forcing amplitudes. $\epsilon(f^*)$ is found to decrease with frequency since a part of energy is dissipated at each scale while another part is transferred to higher frequency. Thus, the theoretical scenario of weak turbulence where all the energy should be dissipated for frequencies larger than a critical dissipative frequency f_d (see Fig. 8) is not realistic in our experiments. A nonconstant energy flux through the scale has been also found numerically in wave turbulence on a metallic plate in the presence of dissipation at all scales [7].

The mean energy flux ϵ^* is then defined by the energy flux averaged through the capillary frequency range

$$\epsilon^* = \frac{\int_{f_{gc}}^{f_d} \epsilon(f)\,df}{f_d - f_{gc}}. \tag{19}$$

Figure 8 shows the mean energy flux ϵ^* for different forcing amplitudes [see the (•) symbols]. These values roughly correspond to values of $\epsilon(f)$ at $f \approx 80$ Hz in the middle of the cascade. The inset of Fig. 8 shows the evolution of ϵ^*, the values of the flux at the beginning, $\epsilon(f_{gc})$, and at the end, $\epsilon(f_d)$, of the capillary cascade as a function of the dissipated power D_c by capillary waves. Note that from Eq. (18), Eq. (15), and Eq. (12), one has $\epsilon(f_{gc}) = D_c$. These three quantities depend linearly on D_c. Thus, rescaling the wave spectrum with one of these quantities would be equivalent. We choose $\epsilon \equiv \epsilon^*$ as an estimation of the energy flux cascading through the capillary scales. Figure 9 (bottom) then shows the rescaled spectrum $S_\eta/(\epsilon^*)^{1/2}$ where all curves roughly collapse on a single curve.

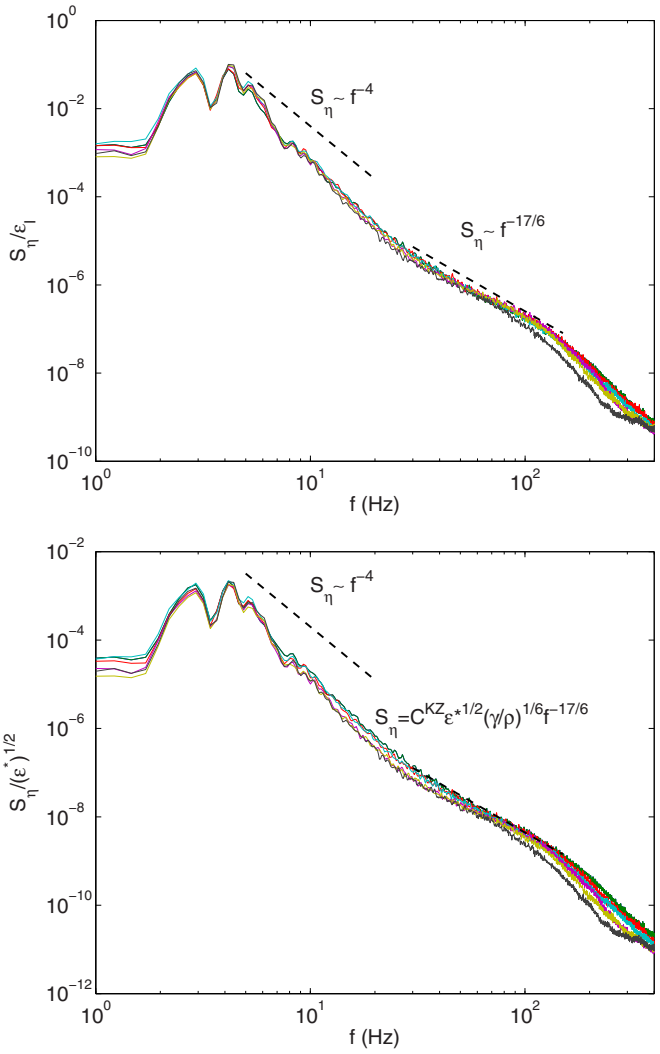

FIG. 9. (Color online) Rescaled power spectrum S_η/ϵ_I (top), and $S_\eta/\epsilon^{*1/2}$ (bottom). In both cases, data roughly collapse on a single curve. Data are the same as in Fig. 2 (top) ($10^{-4} \leqslant \epsilon_I \leqslant 5\ 10^{-4}$ m^3 s^{-3}, mercury). Dot-dashed line: Theoretical capillary spectrum of Eq. (1) with $C^{KZ} = 0.01$. Dashed lines: Theoretical frequency scaling of the spectrum for gravity $S_\eta \sim f^{-4}$ and capillary $S_\eta \sim f^{-17/6}$ wave turbulence.

To sum up, we have shown that dissipation at all scales explains the previous controversy of the scaling of the capillary wave spectrum with the mean energy flux. A new estimation of the flux has been proposed from the dissipated power. The energy flux is then found to be nonconstant over the scales. Nevertheless, the estimation of the mean energy flux allows us to rescale properly the wave height spectrum, and we observe $S_\eta(f) \sim \epsilon^{1/2} f^{-17/6}$ in agreement with the theory of capillary wave turbulence.

VII. ESTIMATION OF THE KOLMOGOROV-ZAKHAROV CONSTANT

In the previous section, we have shown that the scalings of the capillary spectrum both with frequency and with the mean energy flux ϵ^* are found in agreement with wave turbulence theory of Eq. (1). We can thus now evaluate experimentally the Kolmogorov-Zakharov constant C^{KZ} using the estimation $\epsilon \equiv \epsilon^*$. Figure 9 (bottom) shows the Kolmogorov-Zakharov spectrum $S_\eta(f) = C^{KZ}_{\rm exp}\epsilon^{*1/2}(\frac{\gamma}{\rho})^{1/6} f^{-17/6}$, where the constant $C^{KZ}_{\rm exp}$ is experimentally fitted (see dot-dashed line). One finds $C^{KZ}_{\rm exp} \approx 0.01$.

The C^{KZ} constant was previously calculated from the wave action spectrum n_k [17]. The relation between the constants defined from n_k ($C^{KZ}_{n_k}$) and from $S_\eta(f)$ (C^{KZ}) is given by $C^{KZ} = \frac{4\pi}{3} C^{KZ}_{n_k} (2\pi)^{-17/6}$. The $(2\pi)^{-17/6}$ factor is due to the change from frequency f to the pulsation ω, and the $\frac{4\pi}{3}$ factor comes from the relation between n_k and $S_\eta(f)$. Theoretically, $C^{th}_{n_k} = 9.85$ [17], while in the numerical simulations, $C^{n}_{n_k} \approx 1.7$ [17]. The difference between theory and numerics is explained by the small inertial range and the existence of numerical dissipation [17].

Here we experimentally found $C^{KZ} \approx 0.01$, which corresponds to $C^{KZ}_{n_k} \approx 0.5$. This value is 3.4 times smaller than the numerical value and 20 times smaller that the theoretical one. However, we have to keep in mind that dissipation occurs at all scales experimentally, and that a nonconstant energy flux through the scales is observed, contrary to the theoretical hypotheses.

VIII. CONCLUSION

In this paper we have discussed the influence of dissipation on gravity-capillary wave turbulence. We have shown that the main part of the injected energy at a large scale is dissipated by gravity waves and only a small part of it is transferred to capillary waves. This show that evaluating the energy flux by the mean injected power is not a valid approximation. We propose an estimation of the energy flux within the capillary cascade, related to the linear dissipated power by the capillary waves with the cascade inertial range.

A capillary wave turbulence regime with a wave spectrum as a power law of the scale is observed whatever the intensity of the dissipation, but two regimes can be defined, depending on the level of dissipation in the system.

When the dissipation is low enough, the wave spectrum is found in good agreement in regard to the frequency scaling and the energy flux scaling (newly defined). This result explains the previous controversy on the energy flux scaling of the capillary wave spectrum [8,15], pointed out as an open question in a recent review [4]. The Kolmogorov-Zakharov constant is then evaluated experimentally. The value is found one order of magnitude smaller than the one predicted by the theory, since dissipation occurring at all scales is observed experimentally, as well as a nonconstant energy flux through the scales in contrast to the theoretical hypotheses.

When the dissipation goes beyond a certain threshold, the power-law spectrum becomes steeper and the agreement with the theory is lost. The spectrum becomes steeper when the dissipation is further increased. This latter has also been observed experimentally and numerically in flexural wave turbulence [5,7]. It is possible that dissipation is also responsible for the discrepancy between theory and experiment observed in wave turbulence at the surface of a floating elastic sheet [41]. Moreover, at high dissipation, the capillary wave spectrum

is found to depend on the injected power, which reminds us of results in gravity wave turbulence [8,23,34]. Thus dissipation appears to be of prior importance to explain the differences between weak turbulence theory and experimental wave turbulence regimes.

The next step would to explain quantitatively the threshold from the *low dissipation* to the *high dissipation* situations. The measurement of the nonlinear interaction time τ_{nl} and its comparison with the dissipation time should be the starting point. Experimentally, a direct measurement of the energy flux in the k space (in a similar way to what is done numerically [7]) remains an important challenge and would be of interest to confirm our results and discuss the nonlinear time. Moreover, it would be interesting to be able to close the power budget by means of surface and bulk measurements. A better understanding of nonlinear dissipation processes also appears necessary, for wave breaking and the occurrence of ripples on gravity waves. The inclusion of these kinds of coherent structures, as well as the coexistence of dissipation [48] and energy transfers, are important challenges to improve our understanding of natural wave turbulence systems.

ACKNOWLEDGMENTS

We thank C. Laroche for technical help and S. Fauve for discussions. This work has been supported by ANR Turbulon 12-BS04-0005.

[1] V. E. Zakharov, G. Falkovitch, and V. S. L'vov, *Kolmogorov Spectra of Turbulence. I. Wave Turbulence* (Springer, Berlin, Germany, 1992), p. 275.
[2] S. Nazarenko, *Wave Turbulence* (Springer, Berlin, Germany, 2011).
[3] E. Falcon, Discret. Contin. Dyn. Sys. B **13**, 819 (2010).
[4] A. C. Newell and B. Rumpf, Ann. Rev. Fluid Mech. **43**, 59 (2011).
[5] T. Humbert, O. Cadot, G. During, C. Josserand, S. Rica, and C. Touze, Europhys. Lett. **102**, 30002 (2013).
[6] G. During, C. Josserand, and S. Rica, Phys. Rev. Lett. **97**, 025503 (2006).
[7] B. Miquel, A. Alexakis, and N. Mordant (unpublished).
[8] E. Falcon, C. Laroche, and S. Fauve, Phys. Rev. Lett. **98**, 094503 (2007).
[9] M. Berhanu and E. Falcon, Phys. Rev. E **87**, 033003 (2013).
[10] B. Issenmann and E. Falcon, Phys. Rev. E **87**, 011001 (2013).
[11] C. Falcón, E. Falcon, U. Bortolozzo, and S. Fauve, Europhys. Lett. **86**, 14002 (2009).
[12] W. B. Wright, R. Budakian, and S. J. Putterman, Phys. Rev. Lett. **76**, 4528 (1996).
[13] E. Henry, P. Alstrom, and M. T. Levinsen, Europhys. Lett. **52**, 27 (2000).
[14] M. Brazhnikov, G. Kolmakov, and A. Levchenko, J. Exp. Theor. Phys. **95**, 447 (2002).
[15] H. Xia, M. Shats, and H. Punzmann, Europhys. Lett. **91**, 14002 (2010).
[16] A. N. Pushkarev and V. E. Zakharov, Phys. Rev. Lett. **76**, 3320 (1996).
[17] A. Pushkarev and V. Zakharov, Physica D **135**, 98 (2000).
[18] R. G. Holt and E. H. Trinh, Phys. Rev. Lett. **77**, 1274 (1996).
[19] D. Snouck, M.-T. Westra, and W. van de Water, Phys. Fluids **21**, 025102 (2009).
[20] J. Blamey, L. Y. Yeo, and J. R. Friend, Langmuir **29**, 3835 (2013).
[21] M. A. Bouchiat and J. Meunier, J. Phys. (France) **32**, 561 (1971).
[22] D. R. Furhman, P. A. Madsen, and H. B. Bingham, J. Fluid Mech. **513**, 309 (2004).
[23] P. Denissenko, S. Lukaschuk, and S. Nazarenko, Phys. Rev. Lett. **99**, 014501 (2007).
[24] L. Deike, M. Berhanu, and E. Falcon, Phys. Rev. E **85**, 066311 (2012).
[25] J. W. Miles, Proc. R. Soc. London A **297**, 459 (1967).
[26] L. Landau and F. Lifchitz, *Mecanique des fluides* (Editions Mir, Moscow, 1951).
[27] H. Lamb, *Hydrodynamics* (Dover, New York, 1932).
[28] W. G. V. Dorn, J. Fluid Mech. **24**, 769 (1966).
[29] D. M. Henderson and J. W. Miles, J. Fluid Mech. **213**, 95 (1990).
[30] G. P. Association, *Physical Properties of Glycerine and Its Solutions* (Glycerine Producers' Association, New York, 1963).
[31] E. Falcon, S. Aumaitre, C. Falcon, C. Laroche, and S. Fauve, Phys. Rev. Lett. **100**, 064503 (2008).
[32] E. Herbert, N. Mordant, and E. Falcon, Phys. Rev. Lett. **105**, 144502 (2010).
[33] P. Cobelli, A. Przadka, P. Petitjeans, G. Lagubeau, V. Pagneux, and A. Maurel, Phys. Rev. Lett. **107**, 214503 (2011).
[34] S. Nazarenko, S. Lukashuk, S. McLelland, and P. Denissenko, J. Fluid Mech. **642**, 395 (2010).
[35] V. E. Zakharov and N. N. Filonenko, Sov. Phys. Dokl. **11**, 881 (1967).
[36] O. M. Phillips, J. Fluid Mech. **4**, 426 (1958).
[37] E. Kartashova, in *Nonlinear Waves and Weak Turbulence*, Series of AMS Translations 2, Vol. 182, edited by V. E. Zakharov (American Mathematical Society, Providence, RI, 1998), pp. 95–130.
[38] V. E. Zakharov, A. O. Korotkevich, A. N. Pushkarev, and A. I. Dyachenko, JETP Lett. **82**, 487 (2005).
[39] S. Nazarenko, J. Stat. Mech. (2006) L02002.
[40] V. S. L'vov and S. Nazarenko, Phys. Rev. E **82**, 056322 (2010).
[41] L. Deike, J.-C. Bacri, and E. Falcon, J. Fluid Mech. **733**, 394 (2013).
[42] A. I. Dyachenko, A. O. Korotkevich, and V. E. Zakharov, JEPT Lett. **77**, 477 (2003).
[43] W. K. Melville, F. Veron, and C. J. White, J. Fluid. Mech. **454**, 203 (2002).
[44] G. Chen, C. Kharif, S. Zaleski, and J. Li, Phys. Fluids **11**, 121 (1999).
[45] A. V. Fedorov and W. K. Melville, J. Fluid Mech. **354**, 1 (1998).
[46] W.-T. Tsai and L.-P. Hung, J. Phys. Oceanogr. **40**, 2435 (2010).
[47] G. Caulliez, J. Geophys. Res. **118**, 672 (2013).
[48] A. Newell and V. Zakharov, Phys. Lett. A **372**, 4230 (2008).